Published in final edited form as:
IEEE Trans Biomed Eng. 2008 ; 9: 314–317. doi:10.1109/ISBI.2012.6235547.

INTERVENTIONAL MRI WITH SPARSE SAMPLING USING UNION-OF-SUBSPACES

S. Derin Babacan, **Fan Lam**, **Xi Peng**, **Minh N. Do**, and **Zhi-Pei Liang**
Beckman Institute for Advanced Science and Technology, and, Department of Electrical and Computer Engineering, University of Illinois at Urbana-Champaign

Abstract

A significant problem in interventional magnetic resonance imaging is limited imaging speed. This paper addresses this problem using a new signal model known as union-of-subspaces. This model enables an effective use of sparse sampling and prior information to significantly improve the imaging speed. The proposed method has been validated using simulations on real interventional imaging data, and is shown to provide high speed and quality imaging. The approach is very flexible and can be applied to other imaging applications as well.

Index Terms

Interventional MRI; fast imaging; sparse sampling; union of subspaces

1. INTRODUCTION

Interventional magnetic resonance imaging (iMRI) has a wide range of potential clinical applications including MR-guided neurological surgery, minimally invasive biopsy, interventional tumor management and vascular stenting [1, 2]. A great technical challenge in iMRI is the need of real time image acquisition and reconstruction at high spatial resolution and low noise levels. This challenge is especially prominent in the presence of physiological motion, surgical and therapeutic events, and contrast changes due to therapy, which occur commonly in interventional procedures. A significant amount of research is being conducted to improve the imaging speed and quality: Technological developments in hardware design and fast pulse sequences [3, 4] permit acquisition at near real-time with relatively high signal-to-noise-ratio (SNR) and resolution. Parallel imaging [5] readily enables significant gains in imaging speed.

In parallel, methods have been proposed based on sparse k-space sampling. Keyhole techniques [6] acquire an initial high resolution reference image before the interventional procedure, which is then linearly combined with the sparse k-space samples acquired during the interventional procedure. In addition, recent advances in image reconstruction, mostly due to the emergence of compressive sensing (CS) in MRI [7], leads to further increases in imaging speed through reduced sampling. However, the MR imaging rates are still far from the desired level in some applications (especially in 3D imaging), and there is a growing need for fast imaging methods without significant compromises in resolution and SNR.

In this work, we present a novel interventional imaging method for fast and high quality acquisition. Our framework is based on image modeling within union-of-subspaces, which is a generalization of a large class of constrained imaging methods. We demonstrate that this framework is especially suitable for iMRI. Specifically, the structural properties of images are constrained to a union-of-subspaces, which is constructed using the substantial amount of prior information extracted from reference scans collected before the interventional procedure. Additionally, we provide methods for alignment of this reference information with respect to the images of interest, and develop a *dynamic* referencing method for challenging dynamic iMRI scenarios. Finally, we propose an efficient algorithm using this framework suitable for fast image reconstruction with minimal latency. The proposed method is able to achieving superior imaging speed with high image quality, and can be used both to increase the imaging speed in current applications and to open up new applications in iMRI that are currently impractical.

The rest of the paper is organized as follows. In Section 2, we present the image modeling within the union-of-subspaces paradigm. We also show how reference information can be systematically incorporated within this framework. We provide some representative results using this framework in Section 3, and conclude in Section 4.

2. PROPOSED METHOD

The proposed method achieves high-speed interventional imaging by sparse sampling in k-space. A high quality image is then recovered from these samples by embedding reference anatomical information in an efficient and robust manner through a novel framework. The components of the proposed methodology are described in the following sections.

2.1. Image Model

We consider Fourier encoded imaging where data acquisition is described by

$$d(\mathbf{k})=\int \rho(\mathbf{r})\, e^{-i2\pi\, \mathbf{k}\cdot\mathbf{r}}\, d\mathbf{r}, \quad (1)$$

where $d(\mathbf{k})$ is the measured data and $\rho(\mathbf{r})$ is the image of interest. Discretizing (1) yields

$$\mathbf{d}=\mathbf{F}_u\, \boldsymbol{\rho}+\mathbf{n}, \quad (2)$$

where $\boldsymbol{\rho} \in \mathbb{C}^N$ and $\mathbf{d} \in \mathbb{C}^M$ are the desired image and measurements as vectors, $\mathbf{F}_u \in \mathbb{C}^{M\times N}$ is the undersampled Fourier encoding matrix with $M < N$, and $\mathbf{n}$ is the observation noise.

Given a set of imaging parameters (pulse sequence, repetition time (TR), etc.), the strategy used in this work to improve the imaging speed is to sparsely sample k-space. However, in this case, the image $\boldsymbol{\rho}$ is sampled below the Nyquist rate and the encoding matrix does not cover the entire space $\mathbb{C}^N$, thus many possible signals are consistent with the same set of measurements. Prior knowledge on the solution should be incorporated to find a unique solution, which typically corresponds to restricting the solution space of $\boldsymbol{\rho}$.

In this work, we consider a general model by assuming that the image function ρ lives in a union-of-subspaces [8, 9], which enables *structural* modeling of images in addition to sparsity. Specifically, the image space $\mathscr{V} \subset \mathbb{C}^N$ is clustered as

$$\mathscr{V} = \bigcup_i \mathscr{V}_i, \quad (3)$$

where $\mathscr{V}_i$ denote the individual subspaces with corresponding bases Ψ_i. The image function $\rho \in \mathscr{V}$ if and only if there is some j for which $\rho = \mathscr{V}_j$, i.e., ρ belongs to one subspace and can be represented as $\rho = \Psi_j \alpha_j$. If the knowledge is available about which subspace $\mathscr{V}_j$ the image function resides in, then reconstruction reduces to inverse projection of the acquired data onto $\mathscr{V}_j$, which is typically performed by solving a least-squares problem. However, such information is not available in most practical settings, and a more involved problem of joint identification of the subspace and reconstruction is required. Without assuming any prior structure on the subspaces, the recovery of the image is extremely challenging as the number of all possible clusterings of the $\mathbb{C}^N$ is prohibitively large (e.g., $\begin{pmatrix} N \\ K \end{pmatrix}$ for K-dimensional subspaces). However, union-of- subspaces model provides the necessary means for specific signal models which allow certain subspaces and remove others from the solution space.

The union-of-subspaces framework can be seen as a generalization of many existing constrained imaging methods. Some examples are given below.

- *Compressive sensing (or sparse representation)* [7]: Here the unknown signal is approximated as being K-sparse, i.e., it can be represented by K basis functions as $\rho = \Sigma_{l \in I} \Psi_{l} \alpha_l$, where I is the index set of K selected bases. Defining $\mathscr{V}_i$'s to be all K-dimensional subspaces of $\mathbb{C}^N$, it can be seen that ρ lives in the subspace $\mathscr{V}_i$ that contains the basis functions indexed with I, and the entire image space is characterized by a union-of-subspaces.

- *Group sparsity:* These approaches generally pre-cluster the presentation basis Ψ into disjoint bases Ψ_i (with the corresponding groups of coefficients α_i) based on some prior knowledge. This prior knowledge is generally in terms of intensity values or connectivity (for instance within wavelet trees or spatial-spectral components [10]). Since each group Ψ_i forms a basis for a subspace $\mathscr{V}_i$, this approach is a special case of the union-of-subspaces modeling.

- *Partial separability* [11]: In these approaches, a spatiotemporal sequence is modeled by $\rho(\mathbf{k}, t) = \sum_{l=1}^{K} \alpha_l \, c_l(\mathbf{k}) \, \phi_l(t)$. Defining the span of the sets $\{c_l(\mathbf{k})\}_{l=1}^{K}$ and $\{\phi_l(\mathbf{k})\}_{l=1}^{K}$ respectively as the spatial and temporal subspaces, we observe again that this formulation constitutes the entire image space as a union-of-subspaces.

It is possible to give more examples. In fact, the union-of-subspaces framework covers a very large class of existing image models, and, in addition, offers many new modeling options and enhanced flexibility in incorporating prior knowledge in image reconstruction.

In this work, we show that the union-of-subspaces modeling provides a powerful framework for interventional imaging via systematic incorporation of prior knowledge. In most interventional imaging applications, a reference image ρ^R (or a collection of reference images) can be obtained before the intervention procedure without strict restrictions on the imaging parameters. Within the union-of-subspaces framework, appropriate utilization of these reference images allow both for (i) identifying the subspace $\mathcal{V}_*$ the target image is expected to belong to, and for (ii) restricting the energy distribution within this subspace, hence the relative importance of components of this subspace.

In the following, we provide details on how prior information from reference images can be embedded into interventional imaging using union-of-subspaces modeling in a robust manner.

2.2. Identifying the Image Subspace

The main advantage of the union-of-subspaces based formulation is to enforce structural constraints. The key to achieving high quality reconstructions is appropriate structural clustering of the image space into subspaces, and identifying the subspace in which the image is expected to exist. Since the general anatomical information observed in the reference image is expected to be approximately the same in the target image, this information can be used for identifying the subspace for the images of interest. Specifically, we first find the sparse representation of the reference image ρ^R in an overcomplete wavelet basis Ψ such that $\rho^R = \Psi\,\alpha^R$. The image subspace is then specified as the span of columns of Ψ that correspond to the nonzero coefficients in α^R, that is

$$\mathcal{V}_* = \mathrm{span}\left(\{\Psi_l\}_{l \in I}\right), \quad (4)$$

with I the index set of basis vectors with nonzero coefficients. We denote $\mathcal{V}_*$ as the image subspace. Instead of forming a basis for it, we use the retained subset of columns of Ψ for its representation, which is denoted by $\tilde{\Psi}$.

2.3. Constraining Relative Energy Distribution within the Image Subspace

As mentioned earlier, with the image subspace defined, the image reconstruction reduces to projecting the acquired data onto this subspace, which amounts to

$$\hat{\boldsymbol{\alpha}} = \arg\min_{\boldsymbol{\alpha}} \left|\left|\mathbf{d} - \mathbf{F}_u\,\tilde{\boldsymbol{\Psi}}\,\boldsymbol{\alpha}\right|\right|_2^2 \quad (5)$$

$$= \left(\tilde{\boldsymbol{\Psi}}^H\,\mathbf{F}_u^H\,\mathbf{F}_u\,\tilde{\boldsymbol{\Psi}}\right)^{-1}\tilde{\boldsymbol{\Psi}}^H\,\mathbf{F}_u^H\,\mathbf{d}. \quad (6)$$

However, solely constraining the solution to the subspace $\mathcal{V}_*$ without further restrictions does not generally provide high image quality.

In addition to specifying the image subspace, the reference image provides information about the structure of this subspace as well. Specifically, via the representation coefficients

$\tilde{\alpha^R}$ that satisfy $\tilde{\Psi}\tilde{\alpha^R} = \rho^R$, it provides information about the energy distribution within this subspace. Since the general anatomical structure among the images are assumed to be approximately same, this subspace structure can be used effectively for further constraining the image reconstruction.

To this end, we first cluster the representation coefficients $\tilde{\alpha^R}$ according to their magnitudes using a K-means algorithm into S classes (typically S = 25), such that $\tilde{\boldsymbol{\alpha}}^R = \sum_{i=1}^{S} \tilde{\boldsymbol{\alpha}}_i^R$. The energy distribution within the subspace is then specified by the relative energy content of these clusters, expressed by the magnitude of the coefficients $\tilde{\boldsymbol{\alpha}}_i^R$. The clustering information and the corresponding energy distribution can then be used as a prior information to constrain (6). Specifically, using the same clustering of $\tilde{\alpha^R}$ on the unknown coefficient vector as $\boldsymbol{\alpha} = \sum_{i=1}^{S} \boldsymbol{\alpha}_i$, we employ an l_2-regularization in (5) as

$$\hat{\boldsymbol{\alpha}} = \arg\min_{\boldsymbol{\alpha}} \frac{1}{\sigma^2} \left|\left| \mathbf{d} - \mathbf{F}_u \tilde{\boldsymbol{\Psi}} \boldsymbol{\alpha} \right|\right|_2^2 + \sum_{i=1}^{S} \lambda_i \left|\left| \boldsymbol{\alpha}_i \right|\right|_2^2 \quad (7)$$

$$= \left(\tilde{\boldsymbol{\Psi}}^H \mathbf{F}_u^H \mathbf{F}_u \tilde{\boldsymbol{\Psi}} + \sigma^2 \boldsymbol{\Gamma} \right)^{-1} \tilde{\boldsymbol{\Psi}}^H \mathbf{F}_u^H \mathbf{d}, \quad (8)$$

where σ^2 is the noise variance and Γ = diag (λ_i), with each λ_i repeated c_i times where c_i is the number of coefficients in cluster i.

The parameters λ_i represent the strength of the enforced regularization on each cluster, and when λ_i assume very large values all coefficients in the corresponding cluster are suppressed. It is evident that regularization should be enforced more heavily on clusters with smaller energy, and lightly on important clusters with high signal energy. Using the energy distribution of the clusters in the reference image, the proposed method employs the following selection of weights

$$\lambda_i = \frac{c_i}{\left|\left| \tilde{\boldsymbol{\alpha}}_i^R \right|\right|_2^2}. \quad (9)$$

Using (9) can be interpreted as adjusting the regularization strength on the clusters according to their relative importance in the reference images. Notice also that via the use of (9), the problem (8) can be solved very efficiently with a single application of the conjugate gradient method. This property significantly reduces the computation time of the algorithm, and enables fast reconstruction required during interventional procedures.

2.4. Incorporating Robustness Against Motion

It is clear that the reference images and the image of interest should be appropriately registered in order to properly translate the prior knowledge on the subspace structure and their relative energy into the reconstruction process.

NIH-PA Author Manuscript

NIH-PA Author Manuscript

In the proposed method, we consider two complementary strategies to account for motion. First, for global motion differences between the images, we employ the rigid motion estimation method in [12] that estimates affine motion parameters using the reference image and the sparse sampled k-space data. Specifically, assuming a parametric motion operator **T** between the reference image ρ^R and the image of interest ρ, such that $\rho \approx \mathbf{T}\rho^R$, we find the motion parameters by solving

$$\hat{\mathbf{T}} = \arg\min_{\mathbf{T}} \left|\left|\mathbf{d} - \mathbf{F}_u\, \mathbf{T}\, \boldsymbol{\rho}^R\right|\right|_2^2. \quad (10)$$

In addition, the global contrast difference can be addressed within this optimization as well [12]. The problem (10) is solved for 6 affine motion parameters using a quasi-Newton method. We observed empirically that global motion is very accurately estimated even at high under sampling factors (e.g., 20).

Physiological motion, e.g., due to respiration, is more complicated than global rigid motion and cannot easily be modeled using parametric models. Our proposal is to follow a data-centric approach: we acquire a collection of reference images temporally $\{\boldsymbol{\rho}_l^R\}_{l=1}^L$ that are representative of the typical physiological motion during the specific intervention. Generally, physiological motion has a quasi-periodic nature, such as respiration or heart movement, and several temporal reference images are able to capture its characteristics. This *dynamic* reference scans can be collected within a period of the anticipated motion via fully-sampled data before the intervention, when the acquisition is not restricted to be fast. In applications when such fully-sampled data that accurately captures the physiological motion cannot be obtained (such as 3D cardiovascular imaging), the dynamic reference can be acquired through use of the advanced image reconstruction methods [13].

After the dynamic reference is acquired, we select for each new acquisition the appropriate reference image ρ^R from this collection which is the closest to the acquired sparse k-space data in the least square sense, that is,

$$\boldsymbol{\rho}^R = \arg\min_{\rho_l^R \in \{\boldsymbol{\rho}_l^R\}_{l=1}^L} \left|\left|\mathbf{d} - \mathbf{F}_u\, \boldsymbol{\rho}_l^R\right|\right|_2^2. \quad (11)$$

2.5. Data Acquisition in the Presence of Prior Information

In this work, we utilize a sampling strategy which acquires both samples from both the low and high frequency regions of k-space, but with different densities. Specifically, each acquisition collects samples from the center portion of k-space with higher density and from the high-frequency portions with lower-density. All spiral, radial and cartesian sampling schemes can be used with this scheme. The motivation behind variable density sampling is the well-known energy distribution characteristics in k-space. However, the sampling is not restricted solely to the low-frequency portion, as deviations from prior knowledge (mostly corresponding to contrast agents, catheter and needles) are captured by both low and high frequency samples.

3. EXPERIMENTAL RESULTS

The proposed framework and algorithm are very flexible and can be applied in many different imaging scenarios. Here we demonstrate its capabilities by simulations using a real active catheter interventional MRI data obtained during an RF electrode insertion in the porcine abdomen (in vivo). The fully-sampled dataset has a matrix size of 384 × 512, and exhibits significant physiological motion due to respiration. Additionally, we introduce global motion between temporal frames via random rotation and translations. Two fully-sampled frames are shown in Fig. 1(a) and (b).

For the proposed method, we use the first 10 frames as the dynamic reference, which captures approximately one respiration period. One of the reference images is shown in Figure 1(a). The global motion between the reference images and the acquired sparse samples is estimated at each time frame using the affine motion estimation method described in Sec. 2.4. An overcomplete Haar wavelet basis is used for signal representation, with the number of clusters S = 25. The image subspace and the clusters are estimated for each reference image separately.

Sparse k-space data is obtained by Cartesian undersampling in the phase-encoding (PE) direction, at approximately 10 times acceleration factor (number of PE lines = 38). We collect 25 PE lines in central k-space, and the remaining 13 PE lines are distributed uniformly at random in the high-frequency region. The compressive sensing based approach [7] with total-variation and wavelet regularization is used for comparison.

The reconstructed images (corresponding to the frame in Fig. 1(b)) are depicted in Fig. 2(a)–(b), while the relative reconstruction errors $||\rho_{\text{gold}} - \hat{\rho}||_2/||\rho_{\text{gold}}||_2$ over time are shown in Fig. 2(d). It is evident that the proposed method consistently provides high recovery performance even at this high undersampling ratio. Both global image features and details around the catheter tip are faithfully reconstructed compared to the gold standard (see Fig. 3). In addition, the image quality is not affected due to the global and physiological motion between frames: The global motion is accurately estimated, and the dynamic reference is able to capture the local physiological motion and consistently produce highly relevant reference image for each new frame. On the other hand, while the CS method is able to show moderate performance, the final image quality is not acceptable for practical settings.

As mentioned before, fast reconstruction for visualization is a key requirement in interventional MRI. CS reconstruction requires a number of iterations generally too time-consuming for interactive visualization. In terms of computational requirement and visual quality, the proposed method offers an attractive choice as it involves only a single conjugate gradient solution, while providing high imaging quality. Due to its non-iterative nature, it can readily be employed for real-time visualization via the use of parallel processing.

4. CONCLUSIONS

In this paper, we presented a novel method for high-speed interventional magnetic resonance imaging. The proposed method is based on image modeling within a union-of-subspaces which enables incorporation of prior structural information into constrained image reconstruction. The method is very robust and its computational complexity is suitable for fast reconstruction and visualization. It can also be used in combination with fast sequences and parallel imaging for more powerful imaging performance.

Acknowledgments

This work was supported in part by the Beckman Institute Postdoctoral Fellowship and the following research grants: NIH-P41-RR023953, NIH-P41-EB001977, NIH-1RO1-EB013695-01, and NSF-CCF-0916953.

References

1. Bucker, A.; Katoh, M. CT- and MR-Guided Interventions in Radiology. Springer; 2009. MR-Guided Interventions - Indications, Technique, Pitfalls.
2. Lederman RJ. Cardiovascular interventional MRI. Circulation. 2005; 112:3009–3017. [PubMed: 16275886]
3. Yutzy SR, Duerk JL. Pulse sequences and system interfaces for interventional and real-time MRI. J Magn Reson Imaging. 2008; 27:267–275. [PubMed: 18219681]
4. Ratnayaka K, Faranesh A, Guttman M, Kocaturk O, Saikus C, Lederman R. Interventional cardiovascular magnetic resonance: still tantalizing. J Cardiovascular Magn Reson. 2008; 10(1):62.
5. Ying L, Liang Z-P. Parallel MRI using phased array coils. IEEE Signal Processing Mag. 2010; 27(4):90–98.
6. Duerk JL, Lewin JS, Wu DH. Application of keyhole imaging to interventional MRI: A simulation study to predict sequence requirements. J Magn Reson Imaging. 1996; 6(6):918–924. [PubMed: 8956138]
7. Lustig M, Donoho D, Pauly JM. Sparse MRI: The application of compressed sensing for rapid MR imaging. Magn Reson Med. Dec; 2007 58(6):1182–1195. [PubMed: 17969013]
8. Lu YM, Do MN. Sampling signals from a union of subspaces. IEEE Signal Processing Mag. 2008; 25(2):41–47.
9. Eldar YC, Mishali M. Robust recovery of signals from a structured union of subspaces. IEEE Trans Inform Theory. 2009; 55(11):5302–5316.
10. Usman M, Prieto C, Schaeffter T, Batchelor PG. k-t group sparse: A method for accelerating dynamic MRI. Magnetic Resonance in Medicine. 2011
11. Liang Z-P. Spatiotemporal imaging with partially separable functions. NFSI-ICFBI 2007. 2007:181–182.
12. Lam F, Haldar JP, Liang Z-P. Motion compensation for reference-constrained image reconstruction from limited data. ISBI. 2011:73–76.
13. Christodoulou AG, Zhao B, Zhang H, Ho C, Liang ZP. Four-dimensional MR cardiovascular imaging: Method and applications. EMBC. 2011:3732–3735.

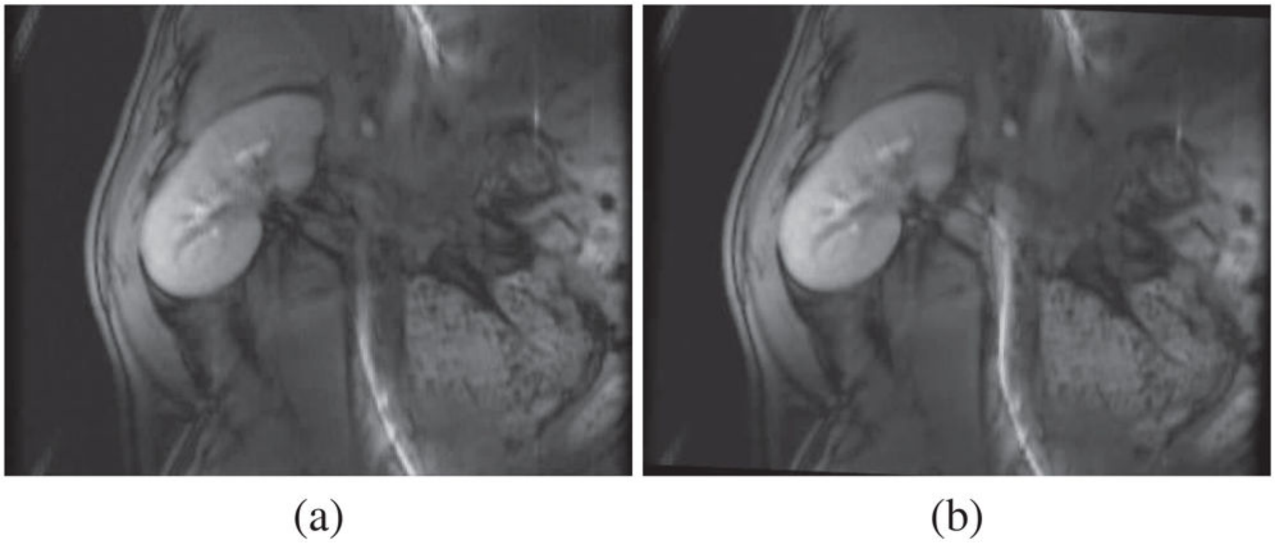

Fig. 1.
(a) A reference scan used in the proposed method and (b) a fully-sampled image (frame 64).

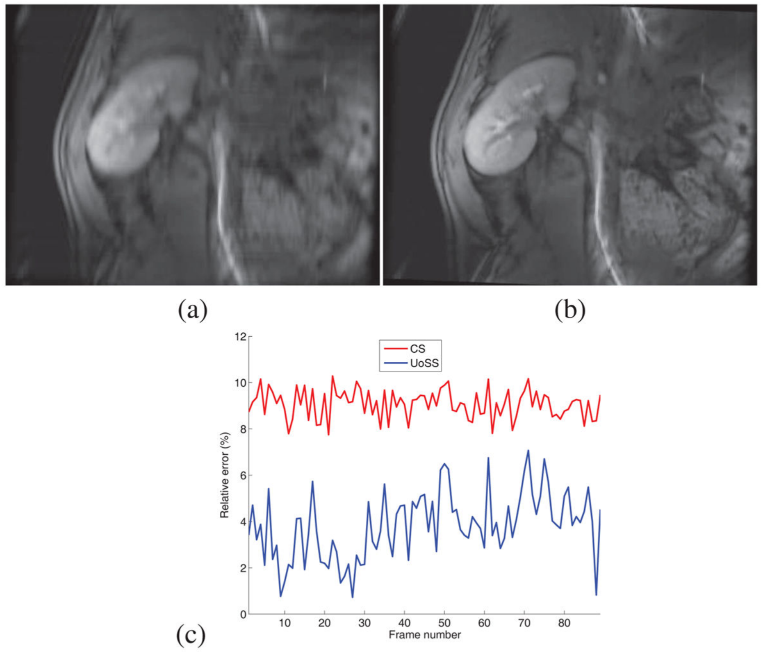

Fig. 2.

Reconstructions using (a) CS and (b) the proposed method (UoSS). The corresponding relative reconstruction errors are 8.6%, and 2.8%, respectively. Relative reconstruction errors for all frames are shown in (c).

NIH-PA Author Manuscript

NIH-PA Author Manuscript

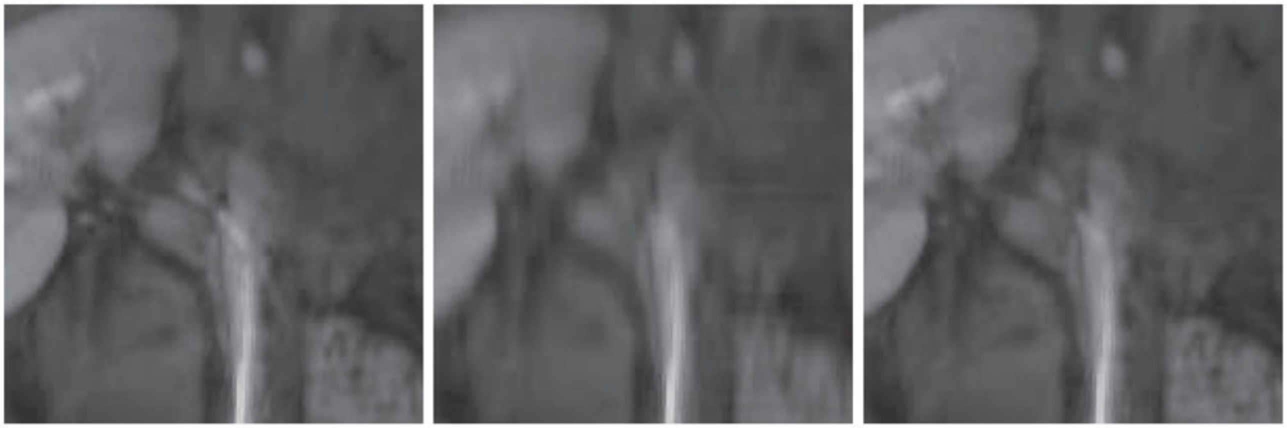
(a) (b) (c)

Fig. 3.
Detailed regions around the catheter tip in the (a) gold standard image, and in the reconstructed images using (b) CS and (c) the proposed method.